Seismological studies of ZZ Ceti stars

2009 J. Phys.: Conf. Ser. 172 012068

(http://iopscience.iop.org/1742-6596/172/1/012068)

Journal of Physics: Conference Series **172** (2009) 012068 doi:10.1088/1742-6596/172/1/012068

Seismological studies of ZZ Ceti stars

B G Castanheira[1,2] and S O Kepler[2]

[1]Institut für Astronomie, Türkenschanzstr. 17, A-1180 Wien, Austria
[2]Departamento de Astronomia Universidade Federal do Rio Grande do Sul, Av. Bento Gonçalves 9500, Porto Alegre 91501-970, RS, Brazil

E-mail: castanheira@astro.univie.ac.at

Abstract. We calculate an extensive adiabatic model grid for pulsating white dwarfs with H dominated atmospheres, the ZZ Ceti stars. We developed a new approach for asteroseismology, using the relative observed amplitudes as weights, and compared the computed modes with the observed ones for the class of ZZ Ceti stars. We measure the H layer mass for 83 stars and found an average of $M_H/M_* = 10^{-6.3}$, which is thinner than the predicted value of $M_H/M_* = 10^{-4}$. Our results indicate that the stars lose more mass during their evolution than previously expected.

1. Introduction

White dwarfs are the final evolutionary stage of almost all stars (95–98%, e.g., Fontaine et al. 2001). Their evolution is basically dominated by cooling. As they cool down, because of the κ-γ mechanism and/or convection driving, white dwarfs pulsate in three different instability strips, depending on the chemical element that drives pulsation. The 143 currently known DAVs (or ZZ Ceti stars) have hydrogen atmospheres and are confined in an observational instability strip between 10 800 and 12 300 K. Recent observations (Castanheira et al. 2007 and Kepler et al. 2006) indicate that pulsation is a phase every white dwarf goes through, i.e., the properties we measure for pulsators can be applied to all white dwarfs. The other two classes are the DBVs, with helium-rich atmospheres, and the DOVs, the hotter pulsators, with roughly a dozen of known pulsators in each class. Their temperatures range from 20 000 to 30 000 K and 75 000 to 170 000 K, respectively.

Asteroseismology is the most powerful tool to study stellar interiors and evolution. Pulsations probe the internal structure of the stars, as every mode is an independent measurement. Even from just a few pulsation modes we can estimate fundamental stellar properties, such as stellar mass (Castanheira & Kepler 2008). Moreover, when a large number of modes is observed, the structure of the star can be determined in detail (e.g., Metcalfe 2005). Pulsating white dwarfs constitute the largest population of variable stars, even though we can only detect the nearest ones because of their intrinsic faintness. Despite the relatively small number of known pulsators, their studies have extremely important astrophysical implications.

The ZZ Ceti stars can be separated in three groups: hot, intermediate and cool. The hot ZZ Ceti stars have only a few modes excited to visible amplitudes, all of them with short periods (smaller than 300 s), small amplitudes (from 1.5 to 20 mma), and the power spectrum does not change substantially from season to season. These stars define the blue edge of the ZZ Ceti instability strip. The standard picture is that pulsations start when the partial ionization zone

of hydrogen deepens into the envelope. As the stars cool down, the depth of the convective zone increases, as well as its size. Around 11 500 K there is a sudden deepening of the convection zone in the models; the observed pulsations change in character, with more modes with long and higher amplitudes excited. At temperatures slightly lower than 11 000 K, the stars stop to pulsate, defining the red edge of the ZZ Ceti instability strip. The high amplitudes observed on the cool part of the strip decreases, consistent with an increase of the depth of the convective zone (Brickhill 1991). The cool ZZ Ceti stars show a very rich pulsational spectra of high amplitude modes (up to 30%) and longer periods (up to 1500 s). The modes interfere with each other, causing dramatic changes in the pulsational spectra. There are also a few red edge stars with long periods of low amplitude, representing the stage when the star is ceasing to pulsate. The intermediate ZZ Ceti stars have characteristics between the hot and the cool groups.

2. The seismological models

2.1. Calculating the models

As the internal structure of white dwarfs with $T_{\rm eff} \sim 12\,000$ K has been sufficiently modified due to cooling, stellar contraction, and chemical diffusion, a hot polytrope static model is equivalent to self-consistent models (e.g. Wood 1990).

We used the White Dwarf Evolutionary Code (Lamb & van Horn 1975, Wood 1990) to evolve the starting model until the desired temperature. The equation of state for the core of our models is from Lamb (1974) and for the envelopes from Fontaine, Graboske & van Horn (1977). We used the updated opacity OPAL tables (Iglesias & Rogers 1996), neutrino rates of Itoh et al. (1996), and ML2/α=0.6 MLT (Bohm & Cassinelli 1971). The core evolution calculations are self-consistent, but the envelope was treated separately. The core and the envelope are stitched together, fulfilling the boundary conditions in the interface. The transitions between the layers are consistent with time diffusion, following Althaus et al. (2003).

2.2. Grid dimensions

We calculated an extensive adiabatic model grid for the pulsation modes, varying four quantities: $T_{\rm eff}$, M, $M_{\rm H}$, and $M_{\rm He}$. The whole grid was generated from a starting polytrope of $M = 0.6\,M_{\odot}$, using homology transformations to obtain models with masses from 0.5 to 1.0 $M_{\odot}$, in steps of 0.005 $M_{\odot}$, initially. The effective temperature ($T_{\rm eff}$) varies from 10 600 to 12 600 K, in steps of 50 K. The upper H and He layer mass values are $10^{-4}\,M_{*}$ and $10^{-2}\,M_{*}$, respectively; above these limits, nuclear reactions would excite g-mode pulsations in the PNNVs by the ϵ mechanism, which are not observed (Hine 1988). The lower H and He layer mass values are $10^{-9.5}\,M_{*}$ (the minimum H amount to be detected in a DA white dwarf spectra) and $10^{-3.5}\,M_{*}$, respectively.

2.3. Core composition: C/O

Varying the core composition introduces three parameters in the fit: the abundance itself from the uncertain C(α,γ)O reaction rate (Metcalfe 2005) and the two extreme points of the function that better describes the transition zone. We chose a homogeneous core of 50:50 C/O, for simplicity. We calculated a representative model of a star in the middle of the instability strip, $T_{\rm eff}$=11 600 K, with mass close to the DA white dwarfs mean distribution, $M = 0.6 M_{\odot}$ (e.g., Kepler et al. 2007), and canonic values for H and He layer masses, $M_{\rm H} = 10^{-4} M_{*}$ and $M_{\rm He} = 10^{-2} M_{*}$. The change for the three first $\ell = 1$ overtones is only a few seconds when the O core abundance (C is the missing quantity) varies from 0% to 90%!

We also investigated the shape of the transition zones when a Salaris-like profile is used (Salaris et al. 1997). The transition zones between the core and the He outer envelope are in different positions; therefore, the trapped modes in these cavities are different. Because the ZZ Cetis pulsate with only a few modes, we decided to use a fixed homogeneous C/O 50:50 core to decrease the number of free parameters in the fit, but still be consistent with the reaction

rate uncertainty. The price payed for this choice is that the He layer mass determinations are uncertain. The differences in the shape of the transition zone can be compensated by changes in the thickness of the He layer. The Salaris profile introduces a more complicated than a linear decrease of the O profile in the outer layers (see Fig. 2. of Metcalfe 2005). This effect potentially changes the calculated trapped modes in the models.

3. Seismology of individual stars: testing for G117-B15A

Since the discovery of its variability (McGraw & Robinson 1976), G117-B15A was considered the most regular ZZ Ceti. Due to its mode stability, Kepler et al. (2005) measured the rate of change of the main mode at 215 s, with a precision better than 10^{-15} s/s. G117-B15A is the most precise optical clock known.

G117-B15A pulsates with only three independent low amplitude modes, showing also the harmonic of the main mode and linear combinations between the modes (Kepler et al. 1982). In table 1 we list the average values for all periodicities detected in observations with the 2.1 m telescope at McDonald Observatory.

Table 1. All detected periodicities for G117-B15A, with mode labeled as well as the linear combinations and the harmonic of the main mode, which are not fundamental modes of the star.

Period (s)	Amplitude (mma)	identification
215.20	17.36	f1
270.46	6.14	f2
304.05	7.48	f3
107.7	1.65	2×f1
126.2	1.40	f1+f3
119.8	1.30	f1+f2

We used G117-B15A as a test of our seismological analysis for two main reasons. First, this star shows a very simple pulsation spectrum, but more than one mode is excited. Second, there are published seismological studies, which can be used to test the validity of our approach.

Our seismological study starts with a literature search for all available information about the star. Besides more than 30 years of time series photometry (Kepler et al. 2005), there are independent measurements of the atmospheric properties ($T_{\rm eff}$ and $\log g$) of G117-B15A, from different techniques (Bergeron et al. 2004, Koester & Allard 2000, and Wegner & Reid 1991). The differences among the published values can be explained by the intrinsic degeneracy between $T_{\rm eff}$ and $\log g$, which allows more than one combination of solutions.

As our models do not account for the excitation of linear combinations nor harmonics, it is very important to be sure that only normal modes are being used in the fit. For G117-B15A, the modes are identified in table 1 as f_1, f_2, and f_3.

To do seismology, we compared the observed modes ($P_{\rm obs}$) with the computed ones ($P_{\rm model}$) by adding the square of the differences, similar to a χ^2 fit. We choose to weight the periods by pulsation energy, which is proportional to the observed amplitude squared ($w_P \propto A^2$), minimizing the quantity S:

$$S = \sum_{i=1}^{n} \sqrt{\frac{[P_{\rm obs}(i) - P_{\rm model}]^2 \times w_P(i)}{\sum_{i=1}^{n} w_P(i)}} \qquad (1)$$

where n is the number of observed modes and w_P is the weight given to each mode.

Even though our model grid uses the adiabatic approximation and does not provide theoretical amplitudes, our choice to weight our fits is to guarantee that the fit will be always dominated by high amplitude modes. For G117-B15A, the periods and their respective normalized weights are 215.20 s, 270.46 s, and 304.05 s, and 0.13, 1.00, and 0.67.

At first, we have tried $\ell = 1$ for all modes. This choice is supported by previous observations of Robinson et al. (1995) and Kotak, van Kerkwijk, & Clemens (2004). We would have tried higher ℓ values if no solution was found, despite the fact that all chromatic amplitude changes to date indicate the modes are more likely $\ell = 1$ than higher ℓ for all ZZ Ceti stars (e.g., Kepler et al. 2000).

By comparing the observations and the models, we found several families of solution below the cut $S < 1.8$ s (the quadratic sum of the relative uncertainties). Figure 1 shows the possible combinations of $T_{\rm eff}$, M, $M_{\rm H}$, and $M_{\rm He}$ below the S cut off, and the minimum of each family is listed in table 2.

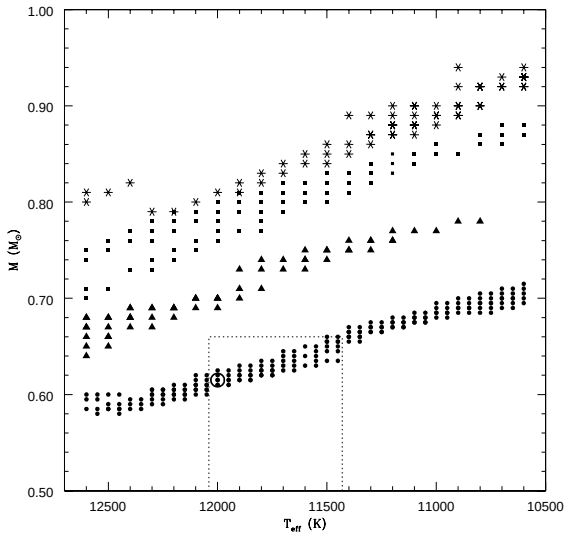

Figure 1. Results from comparison between the pulsation modes of the star G117-B15A and the models. The circles are the solutions for $M_{\rm He} = 10^{-2} M_*$, the triangles for $M_{\rm He} = 10^{-2.5} M_*$, the squares for $M_{\rm He} = 10^{-3} M_*$, and the asterisks for $M_{\rm He} = 10^{-3.5} M_*$. The dotted line box limits the region of the independent temperature and mass determinations ($\pm 1\sigma$) listed in table 2 and the open circle shows the location of the minimum for this family of solutions.

Table 2. Seismological solutions for G117-B15A: absolute minima for each possible family of solution in figure 1.

Symbol in fig. 1	$T_{\rm eff}$ (K)	M ($M_\odot$)	$-\log M_{\rm H}$	$-\log M_{\rm He}$	S (s)	Modes (ℓ, k)
Circles	**12 000**	**0.615**	**7**	**2**	0.67	215.3(1,1), 275.0(1,2) 302.1(1,3)
Triangles	11 500	0.75	5	2.5	0.97	215.1(1,2), 265.1(1,3) 308.0(1,4)
Squares	12 600	0.71	7.5	3	0.73	215.4(1,1), 266.0(1,2) 301.6(1,3)
Asterisks	11 500	0.85	8.5	3.5	0.19	215.2(1,1), 271.5(1,2) 303.3(1,4)

Zhang, Robinson, & Nather (1986) derived the following expression to calculate the uncertainties in the fit parameters: $\sigma^2 = \frac{d^2}{S - S_0}$, where d is the imposed step, S_0 is the absolute minimum, and S is the local minimum in a d difference between the quantities.

The mean uncertainties for the quantities we fit are $\sigma_{T_{\rm eff}} \sim 50\,{\rm K}$, $\sigma_M \sim 0.005\,M_\odot$, $\sigma_{M_{\rm H}} \sim 10^{-0.5}\,M_*$, and $\sigma_{M_{\rm He}} \sim 10^{-0.5}\,M_*$, of the order of the spacings in the model grid. These values are the typical uncertainties in our seismological studies.

The final step is to identify which of the possible solutions correlates with the atmospheric determinations. From external determinations, mass should be between $0.46\,M_\odot$ to $0.66\,M_\odot$, which excludes all seismological high mass solutions; only the first solution in table 2 is consistent with the previous atmospheric determinations. In the same way, the spectroscopic temperature is within the range 11 430 to 12 040 K, which also agrees with this solution. Our seismological solution indicates that $T_{\rm eff}$ is hotter than determined by Bergeron et al. (2004), but consistent with the value from the UV spectra (Koester & Allard 2000).

Alternatively to our procedure, Bradley's (1998) first step is to select seismological models consistent with spectroscopic mass and temperature. He uses a standard model with $M_{\rm He} = 10^{-2}\,M_*$ and C/O nominal profile. Afterwards, he adjusts $M_{\rm H}$ to obtain a mode with $\ell = 1$, $k = 1$ or 2 close to 215 s. Then, he refines $T_{\rm eff}$ and $M_{\rm H}$ to bring the 270 s mode into agreement. The next step is to use the 304 s mode to adjust C/O profile. Finally, he refines the adjustment even more and/or applies small changes to $M_{\rm H}$, $M_{\rm He}$, and in the core structure. He found that the mass of the H layer is either $M_{\rm H} = 10^{-4}\,M_*$ or $10^{-7}\,M_*$, depending if the 215 s $\ell = 1$ mode is $k = 2$ or 1, respectively.

The code he used to calculate his models is basically the same as ours. However, his version used the trace element approximation, while our updated version uses a parameterization that mimics the results of time-dependent diffusion calculations (Althaus et al. 2003) to describe the transition zones. The biggest advantage of our seismological recipe is that we can explore all possibilities, avoiding local minima and error propagation if the spectroscopic determinations are uncertain.

Benvenuto et al. (2002) used realistic He, C, and O profiles, calculated from previous stellar evolutionary phases, obtaining $T_{\rm eff} = 11\,800\,{\rm K}$, $M = 0.525\,M_\odot$, and $M_{\rm H} = 10^{-3.83}\,M_*$, for G117-B15A. Their $T_{\rm eff}$ and mass are consistent with Koester & Allard (2000) determinations by fitting the UV spectrum.

Our seismological study of G117-B15A is in agreement with other approaches, encouraging us to apply the same technique to other ZZ Cetis.

4. Seismology of ZZ Ceti stars by groups

The motivation of grouping the stars is to use the similarities to lower the uncertainties. For stars with similar temperature, mass, and excited modes, it is reasonable to expect that their internal structure would be similar as well. Our approach is akin to having several independent measurements for one particular star.

Our first task was the identification of all periodicities known for all ZZ Ceti stars. We re-analyzed the light curves of the stars observed at the 2.1 m telescope at McDonald Observatory for other projects, like the search for new ZZ Ceti stars conducted by Mukadam et al. (2004), Mullally et al. (2005), and Castanheira et al. (2006), and the search for extra-solar planets orbiting ZZ Ceti stars with stable modes (Mullally et al. 2008), and also for the new ZZ Ceti stars discovered with the 4.1 m telescope SOAR and the 1.6 m telescope at Observatório Pico dos Dias (Kepler et al. 2005b, Castanheira et al. 2006, 2007). The other ZZ Ceti periods were obtained from the literature.

We separate the blue edge ZZ Ceti stars according to the excited mode with highest amplitude. We compared the observed modes with our model grid in the same way as for G117-B15A. We searched for common properties to characterize a particular group, as each group is a specific evolutionary stage in the white dwarf cooling.

83 ZZ Ceti stars have been selected from the SDSS sample. SDSS spectra for $g \leq 18$ stars have S/N$\sim$ 30, and therefore, temperature and mass are reasonably well determined (Kepler et

al. 2006). However, this is not the case for stars fainter than $g = 18$. Bergeron et al. (1995, 2004) followed by Gianninas, Bergeron, & Fontaine (2005) discussed that only with spectra S/N≥70 one can obtain precise temperature ($\Delta T_{\rm eff} \simeq 300\,{\rm K}$) and gravity determinations ($\Delta \log g \simeq 0.1$). Their uncertainties are the external estimates, by fitting the H line profiles of duplicate spectra. The published uncertainties from SDSS spectra are the internal values, obtained by fitting the whole spectrum, combined with colors (see Eisenstein et al. 2006 for detailed explanation). The external uncertainties by comparing duplicated SDSS spectra are of order of 300 K (Kleinman et al. 2004, Eisenstein et al. 2006, Kepler et al. 2007). Kepler et al. (2006), comparing SDSS and Gemini (S/N≥ 70) spectra, found $\Delta T_{\rm eff} \simeq 320\,{\rm K}$, systematically lower in SDSS and $\Delta \log g \simeq 0.24$ dex, systematically larger in SDSS.

Koester & Allard (2000) used UV spectra instead of optical, which results in a higher mass uncertainty, but much better temperature determination. An additional external uncertainty comes from the differences in the model grids from Kiel (e.g. Koester et al. 2001) and Montreal (e.g. Bergeron et al. 2004), which is around 200 K, using a similar line profile fitting technique (Bergeron et al. 2004).

We used the external temperature and mass determinations as a guide for the search of the best among all the possible families of seismological solutions.

5. Results and discussions

We have built an extensive model grid, which calculates all possible modes that can be excited for a given internal structure at certain temperatures. We have also developed an independent technique of model fitting to compare the observed to the calculated periods. In our approach, we used the external temperature and mass determinations to guide the seismological solutions, but we never limited the search to the uncertainty range of the spectroscopic determinations. G117-B15A was the best star to test our seismological approach.

In our seismological study of a few ZZ Ceti stars, seismology was proven to be really a powerful tool in the study of stellar evolution. Even for stars with few excited modes, it is possible to determine some characteristic of their interior. For G226-29, with only one detected mode, it was possible to restrict the mass to be above $0.7\,M_{\odot}$. Combined with reliable values for temperature and mass, three internal parameters could be determined, because the modes do not show an asymptotic behavior, i.e., they are more sensitive to the structure of the star.

The study of G185-32 was the motivation to include the relative amplitudes to give weights to the observed periods in the fits. The idea is that the high amplitude modes should be present in the best models. Our conclusion is that the observed amplitudes should be taken into account, even when one calculates the modes from an adiabatic model.

In the red edge, we studied HL Tau76 and G29-38. For the first, the period spacing was a very useful tool, especially because of the asymptotic behavior of the modes when they are larger. This analysis was consistent with the relative amplitudes between the $\ell = 1$ and 2 modes. In the case of G29-38, we suspected that the spectroscopic solutions were wrong, but we have obtained the same temperature and mass from our seismological study. It was a nice surprise that spectroscopy was right, agreeing with seismology, and that our prejudice that G29-38 should be in the red edge, wrong.

We also studied BPM37093, a high mass white dwarf with $1.1\pm0.05\,M_{\odot}$ (e.g., Bergeron et al. 2004), that has a significant crystallized portion. Even though it was not possible to determine the He layer mass, we could constrain the total stellar masses as high ($M > 1\,M_{\odot}$), temperatures between 11 600 and 11 800 K (only 200 K of external uncertainty), and H layer mass between $10^{-6}\,M_{*}$ and $10^{-7}\,M_{*}$, consistent with seismological determinations from Althaus et al. (2003). Our seismological determinations for the high mass red edge $T_{\rm eff}$ is also in theoretical and observational agreement with this to be hotter than the low mass red edge.

We found that there are many stars in the red edge that need to be re-observed with time-

resolved photometry to detect more of the excited modes. This will allow us to study their interiors. We have demonstrated that it is possible to do seismology, even when a few modes are detected and/or reliable temperature and mass is available, with a minimum of four parameters. More precise spectroscopy will allow better determinations of the atmospheric parameters of the faint stars, providing two extra measurements. For many years, the red edge stars were relegated to oblivion, because we did not know how to study them.

Another important conclusion is that the H layer mass is not dependent on temperature (see Figure 2), according to Kolmogorov–Smirnov and correlation of coefficients tests. Therefore, there is no evidence for accretion or loss of the external layers, as it happens for Miras, for example, as the H layer mass does not vary univocally with temperature (or age). The mass loss of the external layer could come from the lack of reflectivity of the wave in the external layers, as calculated by Hansen, Winget & Kawaler (1985).

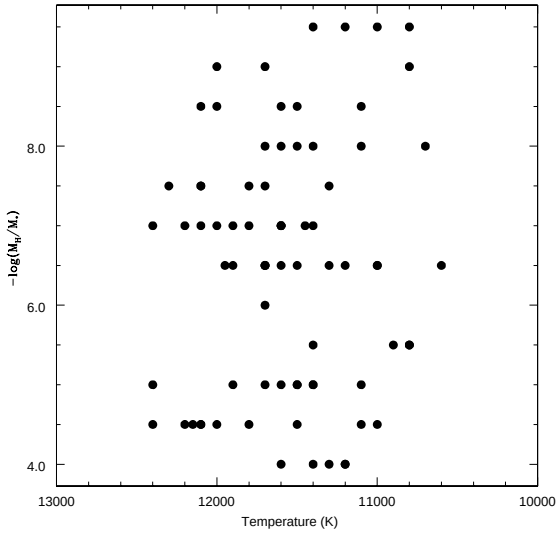

Figure 2. H mass vs. $T_{\rm eff}$, showing that there is no evidence of accretion nor loss of the external layers, as the ZZ Ceti evolves in the instability strip.

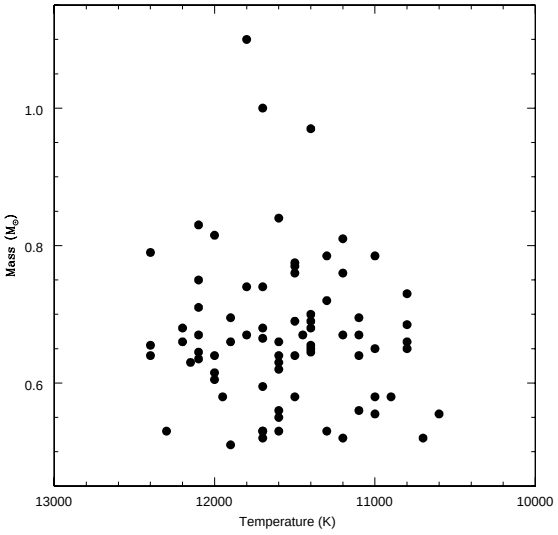

Figure 3. ZZ Ceti instability strip derived from seismology of these stars. We have included just the best solution for each studied star.

The mean value for the H layer mass is $10^{-6.3\pm1.6}\,M_*$, which is different than the canonical value of $10^{-4}\,M_*$, from evolutionary calculations. This result indicates that some white dwarfs, even if their masses are near the most probable value, might have formed with H mass several orders of magnitude smaller than the value predicted by theory, i.e., it is probable that the mass loss during their evolution was, in fact, more efficient than assumed by the models.

Using the seismological results, we derived an auto–consistent instability strip (see Figure 3), which includes the stars from the bright sample and the SDSS stars. This is the first time that the ZZ Ceti stars are studied as a group, by seismology.

We have done the first large seismological analysis of the ZZ Ceti stars as a group, studying 83 stars; before, only 12 ZZ Ceti stars had been studied seismologically. Even though we used the spectroscopic determinations as a guide, we only restricted the seismological solution to the range of spectroscopic parameters if there were not enough modes detected, avoiding local minima to be mistaken as global. After 40 years since the discovery of the first ZZ Ceti star (Landolt 1968), we finally extracted information about this class as a whole.

Acknowledgments
We acknowledge support from the CNPq-Brazil and B. G. C. acknowledges the support from Österreichische Forschungsgemeinschaft. We also acknowledge Travis S. Metcalfe for making available his scripts to calculate the model grid used in this work and Agnes Bischoff-Kim for sharing her version of the model with the Salaris profile. This work has been done with observations from the SOuthern Astrophysical Research telescope, a collaboration between CNPq-Brazil, NOAO, UNC, and MSU.

References
Althaus L G Serenelli A M Córsico A H & Montgomery M H 2003 *A&A* **404** 593
Benvenuto O G Córsico A H Althaus L G & Serenelli A M 2002 *MNRAS* **332** 399
Bergeron P Wesemael F Lamontagne R et al. 1995 *ApJ* **449** 258
Bergeron P Fontaine G Billères et al. 2004 *ApJ* **600** 404
Bohm K H & Cassinelli J 1971 *A&A* **12** 21
Bradley P A 1998 *ApJS* **116** 307
Brickhill A J 1991 *MNRAS* **252** 334
Castanheira B G Kepler S O Mullally F et al. 2006 *A&A* **450** 227
Castanheira B G & Kepler S O 2008 *MNRAS* **385** 430
Castanheira B G 2007 *Ph.D. Thesis* UFRGS-Brazil
Eisenstein D J Liebert J Harris H C et al. *ApJS* **167** 40
Gianninas A Bergeron P & Fontaine G 2005 *ApJ* **631** 1100
Hansen C J Winget D E & Kawaler S D 1985 *ApJ* **297** 544
Hine B P A 1988 *Ph. D. Thesis* UT-Austin
Iglesias C A & Rogers F J 1996 *ApJ* **464** 943
Itoh N Hayashi H Nishikawa A & Kohyama Y 1996 *ApJS* **102** 411
Kepler S O Nather R E McGraw J T & Robinson, E L 1982 *ApJ* **254** 676
Kepler S O Robinson E L Koester D et al. 2000 *ApJ* **539** 379
Kepler S O Costa J E S Castanheira B G et al. 2005a *ApJ* **634** 1311
Kepler S O Castanheira B G Saraiva M F O et al. 2005b *A&A* **442** 629
Kepler S O Castanheira B G Costa A F M & Koester D 2006 *MNRAS* **372** 1799
Kepler S O Kleinman S J Nitta A et al. 2007 *MNRAS* **375** 1315
Kleinman S J Harris H C Eisenstein D J et al. 2004 *ApJ* **607** 426
Koester D & Allard N F 2000 *Baltic Astronomy* **9** 119
Koester D Napiwotzki R Christlieb N et al. 2001 *A&A* **378** 556
Kotak R van Kerkwijk M H & Clemens J C 2004 *A&A* **413** 301
Lamb D Q 1974 *ApJL* **192** L129
Lamb D Q & van Horn H M 1975 *ApJ* **200** 306
Landolt A U 1968 *ApJ* **153** 151
McGraw J T & Robinson E L 1976 *ApJL* **205** L155
Metcalfe T S 2005 *MNRAS* **363** L86
Mukadam A S Mullally F Nather R E et al. 2004 *ApJ* **607** 982
Mullally F Thompson S E Castanheira B G et al. 2005 *ApJ* **625** 966
Mullally F Winget D E Degennaro S et al. 2008 *ApJ* **676** 573
Robinson E L Mailoux T M Zhang E et al. 1995 *ApJ* **438** 908
Salaris M Dominguez I Garcia-Berro E et al. 1997 *ApJ* **486** 413
Wegner G & Reid I N 1991 *ApJ* **375** 674
Wood M A 1990 *Ph.D. Thesis* UT-Austin
Zhang E H Robinson E L & Nather R E 1986 *ApJ* **305** 740